Crossover from fractal capillary fingering to compact flow: The effect of stable viscosity ratios

M. Ferer,* Grant S. Bromhal, and Duane H. Smith*
U.S. DOE, National Energy Technology Laboratory, Morgantown, West Virginia 26507-0880, USA
(Received 26 April 2007; published 4 October 2007)

Using a standard pore-level model, which includes both viscous and capillary forces, we have studied the injection of a viscous, nonwetting fluid into a two-dimensional porous medium saturated with a less viscous, wetting fluid, i.e., drainage with favorable viscosity ratios, $M \geqslant 1$. We have observed a crossover from fractal capillary fingering to standard compact flow at a characteristic time, which decreases with increased capillary number and/or viscosity ratio. We have tested an earlier prediction for the dependence of this crossover upon viscosity ratio and capillary number using our data for a wide-but-physical range of capillary numbers and viscosity ratios. We find good agreement between the predicted behavior and our results from pore-level modeling. Furthermore, we show that this agreement is not affected by changes in the random distribution of pore throat radii or by changes in the coordination number, suggesting that the prediction is universal, i.e., valid for any porous medium structure, as expected from the general nature of the derivation of the prediction. Furthermore, this agreement indicates that the prediction correctly accounts for dependence of the flow upon capillary number and viscosity ratios, thereby enabling predictions for interfacial advance and width as well as saturation and fractional flow profiles. Also this agreement supports the validity of the general theoretical development lending credence to the three-dimensional predictions.

DOI: 10.1103/PhysRevE.76.046304 PACS number(s): 47.56.+r, 47.53.+n, 82.20.Wt

I. INTRODUCTION

A number of essential technologies rely on an understanding of the displacement of one fluid by another in porous media; these include enhanced oil recovery, non-aqueous phase liquid (NAPL) remediation, geologic CO_2 sequestration, and fuel cell operation. Typically the fluid displacements are modeled as a compact (i.e., Euclidean) process whereby the interface advances linearly with the total amount of fluid injected. This assumed behavior is predicted by a Darcy's law treatment using saturation-dependent relative permeabilities [1–3]. However, the flow is known to be modeled by self-similar, invasion percolation fractals in the slow injection limit, i.e., for small capillary number,

$$\mathrm{N_c} = \mu_\mathrm{I} \mathrm{V}/\sigma \approx 0, \tag{1}$$

where μ_I is the viscosity of the more viscous injected fluid, V is the average fluid velocity, and σ is the interfacial tension [4,5]. This invasion percolation model has been widely investigated to determine both its fundamental properties and its predictions for practical problems [4–10].

Several papers have used general theoretical arguments to predict how fractal capillary fingering changes (crosses over) to standard stable-compact-linear flow with increasing capillary number for drainage, where a nonwetting fluid is injected to displace a wetting fluid. The earliest of these predicted that the fractal capillary fingering flows would cross over to compact flows when their linear size exceeded a correlation length, ξ,

$$\xi \propto \mathrm{N_c}^{-\nu/(t-\beta+1+\nu)} \tag{2}$$

where ν, t, and β are the standard percolation theory exponents [11]. Using values of these exponents from two-dimensional percolation theory, the correlation length diverges as the $-\nu/(t-\beta+1+\nu)=-0.3816$ power of the capillary number (0.25 in three dimensions) [12]. Later Xu, Yortsos, and Salin arrived at the same result, while Lenormand as well as Blunt, King, and Scher arrived at numerically similar results [13–15]. Therefore for the case of one-dimensional flow, where the fluid is injected in the x direction at constant rate along one edge of the two-dimensional porous medium, the behavior of the flow will begin to cross over from initial fractal capillary fingering to compact flow when a typical length scale, in the direction of flow (e.g. average distance from the inlet of the interface or of the center of mass, $\langle x \rangle$), becomes greater than the correlation length, $\langle x \rangle > \xi$. For fractal capillary fingering, the fractal dimension, D_f, relates a typical length scale, $\langle x \rangle$ to the volume, V, of injected fluid, which is directly proportional to the time for constant injection rate, $V \propto t \propto \langle x \rangle^{D_f-1}$. Therefore the typical linear extent, ξ, at which a fractal flow begins to cross over to a compact flow, can be related to a characteristic time, τ, at which the crossover begins. For two-dimensional porous media, this yields

$$\tau = \xi^{D_f-1} \propto N_c^{-0.315}, \tag{3}$$

where we have used a recent determination of the value of the fractal dimension for invasion percolation with trapping (IPWT), $D_f=1.825$ [16]. For linear injection along one face of a three-dimensional (3D) porous media, the relationship would be $\tau=\xi^{D_f-2} \propto N_c^{-0.125}$, from the 3D values of the exponents in Eq. (2) and the 3D value of invasion percolation fractal dimension, $D_f \approx 2.525$ [16,17].

*Also at Dept. of Physics, West Virginia University, P.O. Box 6315, Morgantown, WV 26506-6315, USA.

However, this earlier work is incomplete because it did not include the effect of viscosities. The derivation of the correlation length in Xu, Yortsos, and Salin does include the effect of viscosities for general porous media in two and three dimensions [13]. In this work, they derived the following equation [their Eq. (16)] determining the correlation length for a general capillary number and viscosity ratio:

$$\xi^{\nu^{-1}+1}(\xi^{(t-\beta)/\nu} - bM^{-1}) \approx cN_c^{-1}, \tag{4}$$

where

$$M = \mu_I/\mu_D,$$

and where b and c are undetermined constants. It should be noted that we are using Wilkinson's notation. Reference [13] uses σ for correlation length, their viscosity ratio is the inverse of ours, and their exponents are related to the ones in Ref. [11] by $t-\beta=\zeta+\nu(D-2)$.

Assuming equality, this equation becomes

$$\xi^{1.75}(\xi^{0.871} - b/M) = cN_c^{-1}, \tag{5}$$

using values of the percolation exponents in two dimensions. In three dimensions, this equation is $\xi^{2.14}(\xi^{1.77}-bM^{-1}) \approx cN_c^{-1}$. Rearranging the equation for two-dimensional flows, one finds

$$(\xi N_c^{0.3816})^{1.75}[(\xi N_c^{0.3816})^{0.871} - bN_c^{0.332}/M] = c. \tag{6}$$

From this, it is clear that the correlation length will have the scaling form

$$\xi = N_c^{0.3816}\Lambda(\mathrm{b}N_c^{0.332}/M),$$

where $\Lambda(u)$ is a function which can be determined numerically from Eq. (6). Assuming that the leading term $\lambda = \xi(N_c/c)^{0.3816}$ is larger than the term with the viscosity ratio, $u=b(N_c/c)^{0.332}/M$, one can use Eq. (6) to find an expansion in powers of small u, so that the inverse viscosity ratio dependence is given by

$$\xi \approx (c/N_c)^{-0.3816}\{1 + 0.3815u + 0.1368u^2 + \cdots\}, \tag{7}$$

through second-order in the inverse viscosity ratio.

In earlier papers, we had tested the prediction for the capillary number dependence for two-dimensional flows of matched viscosity fluids, showing that the flows exhibited fractal capillary fingering for small t/τ, e.g., the average position of the injected fluid was identical to that from invasion percolation with trapping, $\langle x\rangle/\langle x_{\mathrm{IPWT}}\rangle=1$, and that the flows exhibited compact behavior for large t/τ so that $\langle x\rangle/\langle x_{\mathrm{IPWT}}\rangle \propto t/t^{1/(D_f-1)}$ since the interface as well as $\langle x\rangle$ advances linearly with time for this compact flow [18,19]. The capillary number dependence of the correlation length was also tested in other two-dimensional, matched viscosity studies [20,21]. These tests support the prediction for the capillary number dependence of the crossover from fractal capillary fingering to compact flow. Supporting this prediction of the theory in two dimensions supports the validity of the general theoretical development lending support to the three-dimensional predictions.

It is interesting that the prediction of Ref. [13] indicates that viscosity ratio dependence of the correlation length disappears not only when the capillary number is small but also when the injected fluid has a much larger viscosity than that of the defending fluid. We had previously assumed that the matched viscosity case, $M=1$, would be the cleanest test of Wilkinson's prediction, Eq. (2), because only capillary forces, not the viscous forces, would distinguish between the fluids [11,18]. It appears that other groups may have made the same, seemingly natural assumption by focusing on matched viscosities to study this problem [20,21]. In fact, in an earlier paper, we had attempted, with moderate success, to account for the viscosity ratio dependence of a limited set of data with a power law which increased with viscosity ratio. In this paper, with more extensive data, we show that the form predicted in Eq. (7) describes both the capillary number dependence and the viscosity ratio dependence quite well.

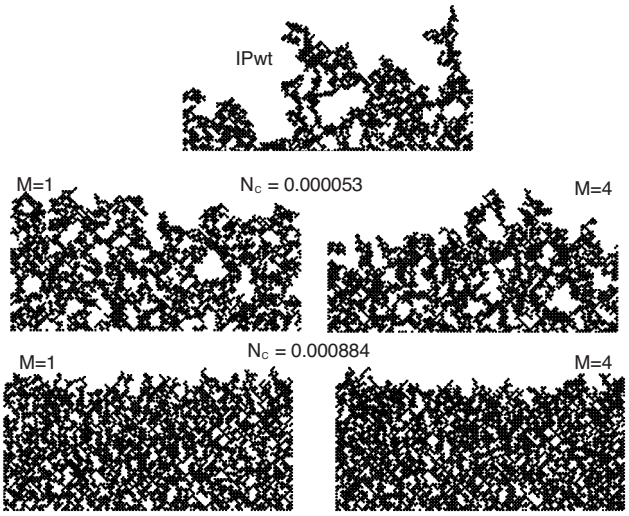

FIG. 1. For two viscosity ratios, typical near breakthrough flow patterns show the progression from invasion percolation with trapping (IPWT) to a relatively small capillary number in the crossover regime to a well-past-crossover capillary number in the compact regime.

II. RESULTS

To test these predictions for the viscosity ratio dependence, we have used results from our standard pore-level model. Our pore-level model has been validated through comparisons with experiment as well as with the invasion percolation with trapping (IPWT) model and diffusion limited aggregation (DLA) model in the appropriate limits [22,23]. Many details of this model have been reported in earlier publications [22,24]; for completeness, we describe some new details of the model essential to this study in the Appendix. Several near-breakthrough patterns of injected fluid occupation are shown in Fig. 1. We have focused on short, wide systems, $W>L$, to improve statistics and to avoid problems observed with coarsening of fractal fingering in long narrow systems, which can lead to spurious linear, i.e., apparently nonfractal, behavior.

Our interest in the displacement efficiency for various technological applications as a function of capillary number

and viscosity ratio has led us to study the dependence of the average position (center of mass) of the injected fluid, ⟨x⟩, as a function of time. The predictions of Ref. [13] can be easily adapted to the behavior of the average position as a function of time. At constant capillary number, i.e., constant volume or mass injection rate for the incompressible fluids, q, the volume, V, of injected fluid is directly proportional to time, $t=V/q$. For fractal fingering, Eq. (3), the linear size of the flow pattern is directly related to the volume of injected fluid, and therefore to the time, by the fractal dimension $V=qt \propto \langle x\rangle^{D_f-1}W$. Inverting, we get the time dependence of the center of mass of the injected fluid,

$$\langle x\rangle \propto (V/W)^{1/(D_f-1)}, \tag{8}$$

where $D_f=1.825$ in two dimensions and $D_f=2.525$ in three dimensions [16,17]. This leads to the definition of time,

$$t = 0.91 + V/W. \tag{9}$$

The additive value 0.91 is merely a fitting constant. For cases of fractal capillary fingering (both for invasion percolation with trapping [10] and for our pore-level modeling for very small capillary numbers), this fitting constant merely shifts the time origin so that the fractal capillary fingering power law behavior, which is already valid at long times without this fitting constant, is also valid at shorter times. At large times, the effect of this constant is negligible. Note that this definition of time allows one to compare systems with different flow velocities and widths but the same capillary number, because this time is related to the real time, t_R, by the q/W factor in capillary number, i.e., $t=0.91+qt_R/W$. Therefore if the crossover occurs when the average position is comparable to the characteristic length, Eq. (7), i.e., $\langle x\rangle \approx \xi$, then the crossover will occur at a characteristic time, τ, given by the fractal relationship between position and time, as in Eq. (8),

$$\tau \propto \xi^{0.825} \approx (c/N_c)^{-0.315}\{1 + 0.3815u + 0.1368u^2 + \cdots\}^{0.825}. \tag{10}$$

To demonstrate the effect of the predicted viscosity ratio dependence in Eqs. (6), (7), and (9), Fig. 2 shows the average position, $\langle x\rangle$, of the injected fluid for one capillary number and several viscosity ratios. These data are normalized to the data for the average position from IPWT, $\langle x_{\mathrm{IPWT}}\rangle$ on the same porous medium realizations, so that the data for the ratio $\langle x\rangle/\langle x_{\mathrm{IPWT}}\rangle$ start from the value unity for small times as will be seen in later figures. Averaging over a number of realizations, these data are plotted both vs time, t, as in Eq. (9) and vs time scaled to the characteristic time in Eq. (10), t/τ on a reduced vertical scale to emphasize the effectiveness of the scaling. The only fitting parameter that was varied to produce this figure is the nonuniversal constant b in the variable $u=b(N_c/c)^{0.332}/M$. The value of b which best collapses the data (grayscale) to one curve is $b=8\pm1$. The predicted characteristic time does account for the viscosity ratio dependence of the data to within reasonable uncertainties.

This is evidence that the predicted viscosity ratio dependence from Ref. [13] does correctly mimic the actual viscosity ratio dependence in the data from our pore level model. It

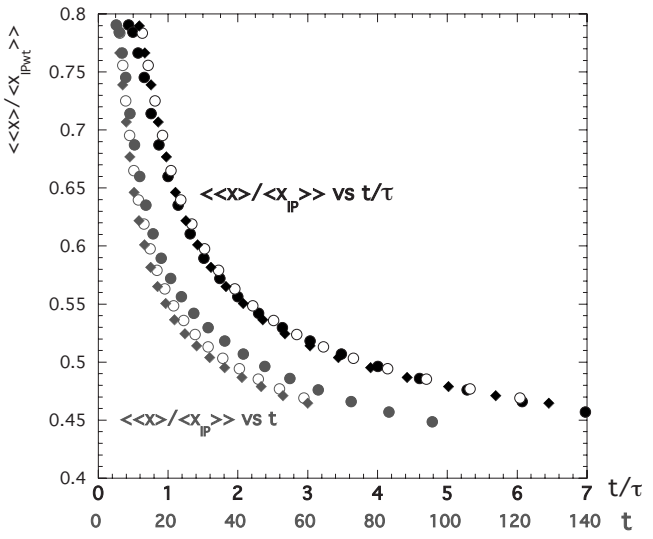

FIG. 2. For the capillary number $N_c=0.000\,885$ and several viscosity ratios [M=1 (closed circles); M=4 (open circles), and M=16 (closed diamonds)], the data for $\langle\langle x\rangle/\langle x_{\mathrm{IP}}\rangle\rangle$ are plotted not only vs time (gray symbols) but also vs time scaled by the characteristic time, Eq. (10) (black symbols).

should also be observed that the unscaled data, i.e., that data plotted vs time, reflect the predicted 1/M dependence, in that the M=16 data differ from the M=4 data by a smaller amount than that by which the M=4 data differ from the M=1 data.

Shown in Fig. 3 are the data for five viscosity ratios (M=1, 2, 4, 8, and 16) and capillary numbers ranging over two orders of magnitude from $N_c=3.5\times10^{-5}$ to 3.5×10^{-3} with

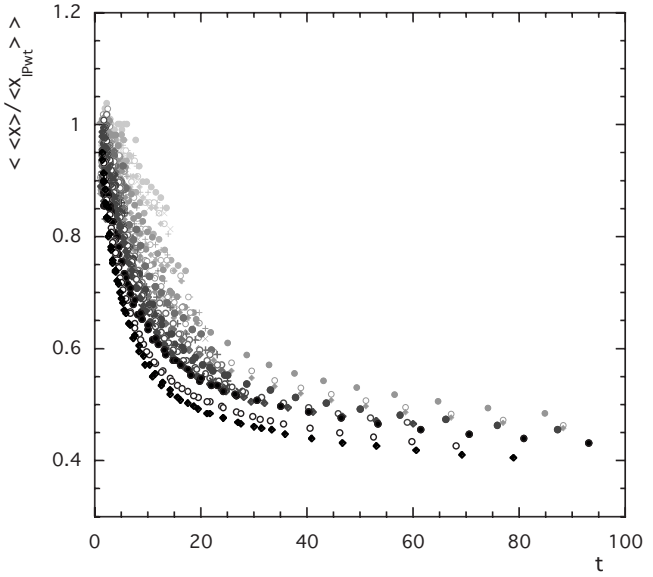

FIG. 3. Plotted vs t are data showing $\langle\langle x\rangle/\langle x_{\mathrm{IPWT}}\rangle\rangle$ for five viscosity ratios [M=1 (closed circles); M=2 (+ symbols); M=4 (open circles); M=8 (× symbols); and M=16 (closed diamonds)]. The gray scale characterizes six different capillary numbers ranging over two orders of magnitude from $N_c=3.5\times10^{-5}$ (lightest gray symbols) to $N_c=3.5\times10^{-3}$ (black symbols).

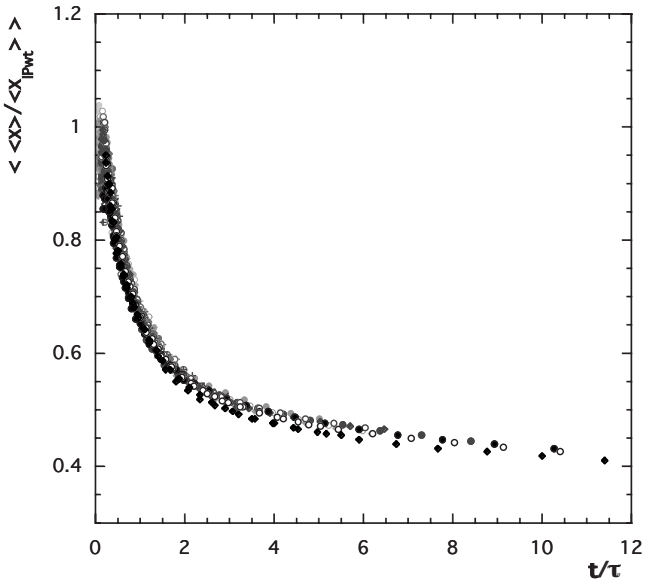

FIG. 4. All of the data from Fig. 3 are plotted vs time scaled by the characteristic time from Eq. (10), using the same value of the fitting parameter, b=8, used in Fig. 2.

the values $N_c=3.5\times10^{-5}$, 1.1×10^{-4}, 2.1×10^{-4}, 4.2×10^{-4}, 8.8×10^{-4}, and 3.5×10^{-3}. Testing the validity of the characteristic time, Eq. (10), as predicted in Ref. [13], Fig. 4 shows all the data in Fig. 3 plotted vs t/τ. In Fig. 4, we use the same value of the nonuniversal constant, b, used in Fig. 2, i.e., $u=8(N_c/c)^{0.332}/M$.

It is clear that the predicted form, with only one adjustable parameter, does indeed collapse the data to one curve. Therefore the predicted characteristic time accounts for the viscosity ratio and capillary number dependence of the flow to within reasonable expectations for the uncertainties in the data. The only consistent deviations occur for the one set of data with the largest value of capillary number, $N_c=3.5\times10^{-3}$, and viscosity ratio, M=16. The scaling predictions, Eqs. (7) and (10) of Ref. [13], predict only the leading singularities in the correlation length and characteristic time. In earlier papers, we had observed deviations in the data for $N_c=3.5\times10^{-3}$ and M=1, which suggests that there is a correction of higher order in capillary number to the M independent and M dependent parts of the characteristic time, which could account for this deviation [18,19].

In these earlier papers, we had explicitly investigated the limiting behavior of the data. For small t/τ, we found that the data for the average position was identical to that for IPWT, i.e., $\langle x\rangle/\langle x_{\mathrm{IPWT}}\rangle=1$. While for large t/τ, the average position increased linearly with time as expected for compact flow, so that $\langle x\rangle/\langle x_{\mathrm{IPWT}}\rangle\propto t/t^{1/(D_f-1)}$. Therefore initially the data exhibited behavior identical to that of fractal capillary fingering and then crossed over to standard compact behavior [18,19]. Since the M=1 data showed the correct limiting forms and since the M>1 data coincides with the M=1 data in Fig. 4, this M>1 data also shows the correct limiting forms of fractal to compact crossover.

In earlier papers testing the Wilkinson prediction for the capillary number dependence, we have shown that this characteristic crossover time, for the crossover from fractal capillary fingering to stable-compact flow, accounts for the capillary number dependence of not only the average position, but also the interfacial width, and the capillary pressure, as well as the saturation and fractional flow profiles [11,18,19]. It seems likely that this extension [13] of the Wilkinson prediction including viscosity ratio will apply equally to all of the same flow properties, since the dependence of these other flow properties upon the characteristic time follows directly from straightforward relationships relating these other properties to the average position [18,19].

III. EFFECTS OF CHANGING THE POROUS MEDIUM STRUCTURE

The above discussion shows that the characteristic time satisfactorily accounts for the capillary number and viscosity ratio dependence of our pore-level modeling of flow in two-dimensional porous media on a diamond lattice [see Fig. 7(a)] with a uniform distribution of the cross-sectional areas of the throats. As with the Wilkinson prediction, the derivation of Eq. (7) was a general scaling argument, which did not depend upon the structure of the porous medium [13]. Therefore we expect that our validation of the prediction for the one two-dimensional porous medium indicates that it should apply equally well to all two-dimensional porous media. To provide evidence supporting this expectation that the leading behavior of the characteristic time is universal, i.e., independent of the detailed structure of the two-dimensional porous media, we have used our pore-level model to study flows in two different porous media structures (see Figs. 7 and 8): (i) a log-normal distribution of pore-throat radii on a diamond lattice and (ii) the same uniform distribution of pore-throat areas as in the previous section, but on a honeycomb lattice (with coordination number three vs the coordination number four diamond lattice). This will test whether the same predicted characteristic time applies to porous media with different distributions of pore-throat radii and with different coordination numbers.

Figures 5(a) and 5(b) show that the characteristic time, Eq. (10), collapses the data for the log-normal distribution of throat radii. Therefore the same characteristic time accounts for both the capillary number dependence and the viscosity ratio dependence of this data for log-normal distributions of throat radii as well as it did for the data in Fig. 3 for the uniform distribution of throat areas. The only difference between the two cases was in the value chosen for the nonuniversal constant; i.e., b=9.5 gave a slightly better data collapse in this case than did the value b=8, used in Fig. 4.

Figures 6(a) and 6(b) show that the characteristic time, Eq. (10), collapses the data for the porous medium with the pore bodies at the sites of a honeycomb lattice. Therefore the same characteristic time accounts for the capillary number dependence and viscosity ratio dependence of the data for this porous medium with coordination number three and of the data in Fig. 3 for a porous medium with coordination number four. The only difference between the two cases was in the value chosen for the nonuniversal constant; i.e., b=9.5 gave slightly better data collapse in this case than did the value, b=8, used in Fig. 4.

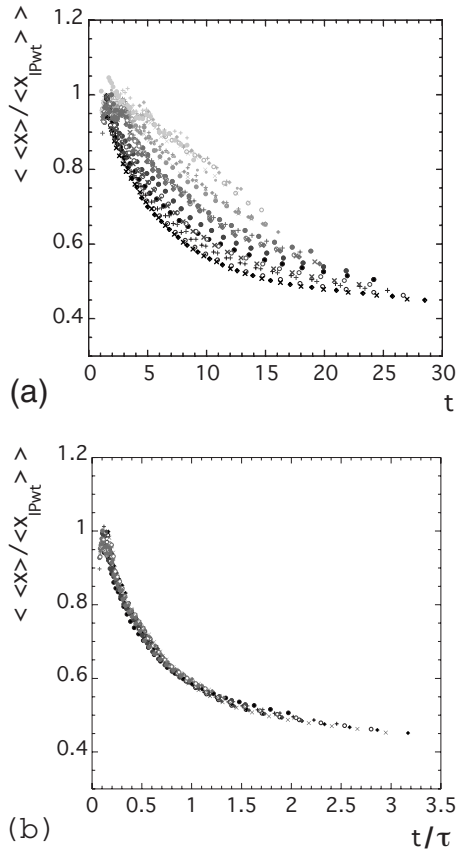

FIG. 5. (a) Data similar to that in Fig. 3. However, this set of data was generated for a log-normal distribution of pore-throat radii connecting pore bodies at the sites of a diamond lattice. (b) Collapse of the data in (a) using the characteristic time in Eq. (10) with a different value of the nonuniversal constant, b.

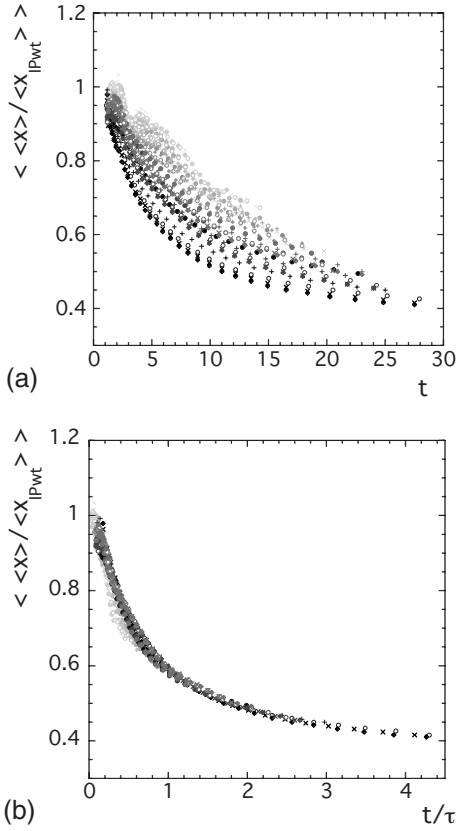

FIG. 6. (a) Data similar to the data in Fig. 3. However, this set of data was generated for an array of pore bodies at the sites of a honeycomb lattice with a uniform distribution of the pore throat areas connecting the pore bodies. (b) The collapse of this data set using the characteristic time in Eq. (10) using the value b=12.

Consistent with the derivation of Ref. [13], we have shown that the same form of the characteristic time, Eq. (10), adequately describes the viscosity ratio and capillary number dependencies of the average position of the injected fluid. This is not to say that the porous media are unimportant. The structure of the porous media does affect a number of important constants involved in the crossover; these include: (i) the constant, Γ, multiplying the power-law dependence of the precrossover average position of the injected fluid, i.e., IPWT, $\langle x_{\mathrm{IPWT}}\rangle = \Gamma t^{1/(D_f-1)}$, (ii) a similar constant, an effective velocity v, in the postcrossover expression for the average position $\langle x\rangle = v\,t$, which is related to the saturation behind the interface, and of course (iii) the constant b. Thus the expressions in Eqs. (7) and (10) do not completely define the crossover for all porous media, but the evidence suggests that they should describe the capillary number and viscosity ratio dependencies for the crossover in any ordinary porous medium.

Because the theoretical arguments of Xu, Yortsos, and Salin are independent of porous media structure, verification of their results for our simplistic porous media structure (uniform areal distribution of throats on a diamond lattice) demonstrates that their arguments are correct for two-dimensional porous media, further supported by our results for log-normal throat distributions and on a hexagonal lattice [13]. Furthermore, because the theoretical arguments, which neglect trapping, are valid in two dimensions where trapping is important, one expects that these arguments should be valid in three dimensions, where trapping is insignificant.

IV. CONCLUSIONS

Using our standard pore-level model, we have demonstrated the validity of the predicted capillary number and viscosity ratio dependence of the characteristic fractal-to-compact crossover time [13], as shown in Eqs. (4)–(10) and Figs. 2–6. Because the derivation of this prediction did not depend upon a particular porous medium structure, validation of the prediction for the two-dimensional porous medium structure in Sec. II indicates that the prediction should be universally valid, i.e., for all two-dimensional porous medium structures. Supporting this assertion, in Sec. III, we demonstrated the validity of the prediction for two different porous media, i.e., one with a log-normal distribution of pore throat radii and another with a different coordination number. More interestingly, our validation of the predictions for two-dimensional porous media argues for the validity of the procedures used to derive the prediction. Since these procedures are independent of dimensionality, one expects that the predictions for three-dimensional porous media should also be valid.

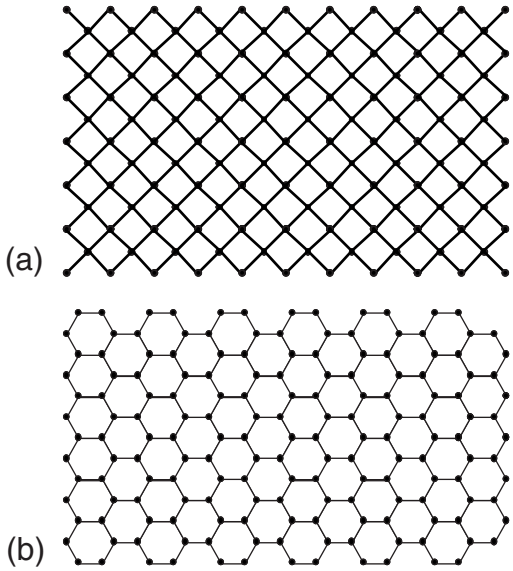

FIG. 7. (a) and (b) show spherical pore bodies connected by throats with randomly chosen cross-sectional area (a) on a diamond lattice with coordination number four shown on the left, and (b) on a hexagonal lattice with coordination number three shown on the right. The length scale for these structures is ℓ, so that the cylindrical throats have length ℓ, the throat radii are in units of ℓ, and the pore-body volumes are all ℓ^3.

Furthermore, having shown that the prediction of Ref. [13] correctly accounts for the capillary number and viscosity ratio dependence of the characteristic time, this expression for the characteristic time can be coupled with arguments from earlier papers predicting the dependence of other flow properties on characteristic time [18,19], which leads to a prediction of the capillary number and viscosity ratio dependence of the interfacial width, the saturation and fractional flow profiles, as well as the effective capillary pressure.

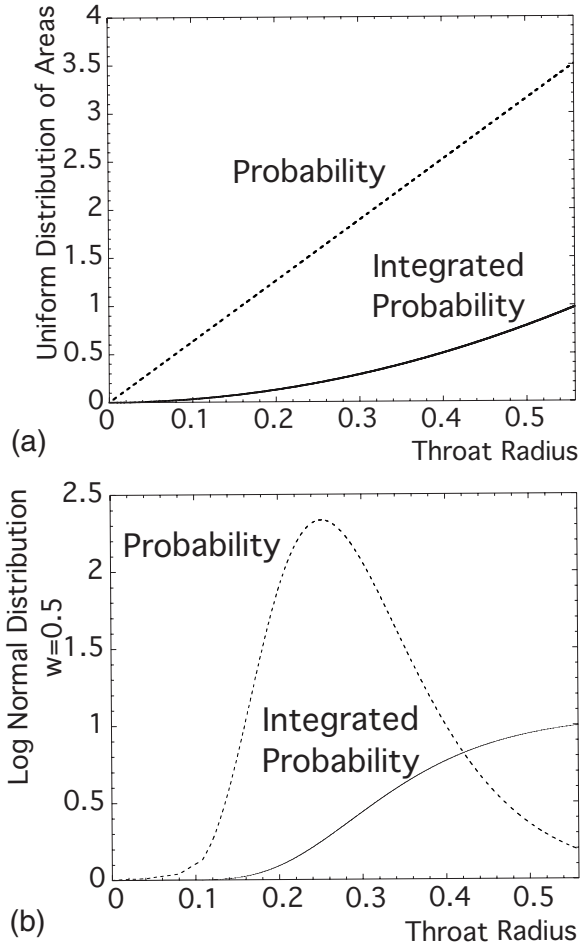

FIG. 8. (a) and (b) show the probability of finding a particular value of the throat radius, r, as well as the integrated or cumulative probability. (a) is for a uniform areal distribution, with areas from 0 to ℓ^2, so that the radii vary from 0 to $\ell/\sqrt{\pi}$. (b) is for a truncated, log-normal distribution with width 0.5ℓ and most probable value of radius, $r=0.2525\ell$, truncated at a maximum value $r=\ell/\sqrt{\pi}$.

ACKNOWLEDGMENT

M. Ferer acknowledges the support of the U. S. Department of Energy, Office of Fossil Energy.

APPENDIX: MODIFICATIONS OF THE POROUS MEDIUM IN THE PORE MODEL

We have developed a computer code to simulate two-phase flow in a model porous medium. In simulating the flow, the computer code includes capillary and viscous forces allowing a study of drainage, where a nonwetting fluid is injected into the porous medium displacing a wetting fluid [22,24]. The simple model of the porous medium consists of spherical pores at the sites of a diamond lattice [Fig. 7(a)]; these pores are connected by cylindrical throats with cross-sectional areas randomly chosen from a uniform distribution, for which the distribution of radii is shown in Fig. 8(a). The model relates the flow velocity through a throat to the pressure drop across the throat modified by any capillary pressure. Conserving volume of our incompressible fluids, a modified Gauss-Seidel iteration is performed to find the pressure field and the resulting flow velocities. The fluids are then advanced in the porous medium using flow rules that we have tried to make as nonrestrictive as possible. This model is a generic pore-level model of the type that has been widely used for the last two decades [7,8,21,25–36]. Although our model has many features in common with these other pore-level models in the literature, there are specific differences, as detailed in previous references [22,24].

Most of our simulations have used this model porous medium of pore bodies at the sites of a diamond lattice connected by throats with cross-sectional areas randomly chosen from a uniform distribution. We did not view this emphasis on one porous medium structure as being restrictive because, consistent with the derivations of Yu *et al.*, and others [11,13–15], we expected that our results would be universal, i.e., insensitive to the details of the structure of the porous medium. To test the validity of this expectation for the case of drainage with stable viscosity ratios, we have modified our computer code to simulate two-phase flow in a regular honeycomb network, with coordination number three, Fig.

7(b). If the behavior of interest is the same for both the diamond and honeycomb networks, then the behavior should be independent of coordination number. Similarly, we have modified our computer code to study flow through a diamond network, with throat radii chosen from a log-normal distribution. As one can see from Figs. 8(a) and 8(b), this distribution is very different from the uniform areal distribution, which gives a linear distribution of radii. If the behavior of interest is the same for both distributions, then the behavior should be independent of the distribution of throat radii. This independence of the essentials of the behavior studied provides support for our expectation of the universality of this behavior. In addition to this work, we have made similar comparisons for two component miscible flows, where we found that the exponent characterizing the leading behavior of the characteristic time was indeed independent of both coordination number and throat distribution [37]. Of course, the characteristic time did depend weakly on porous medium structure through nonuniversal constants, similar to b in Eq. (6) [37].

[1] R. J. Blackwell, J. R. Rayne, and W. M. Terry, Trans. AIME **216**, 1 (1959).
[2] J. Bear, *Hydraulics of Ground Water* (McGraw-Hill, New York, 1979).
[3] F. A. L. Dullien, *Porous Media: Fluid transport and pore structure* (Academic, New York, 1979).
[4] P. Meakin, *Fractals, Scaling, and Growth Far From Equilibrium* (Cambridge University Press, Cambridge 1998).
[5] D. Wilkinson and J. F. Willemsen, J. Phys. A **16**, 3365 (1983).
[6] M. J. Blunt, Curr. Opin. Colloid Interface Sci. **6**, 197 (2001).
[7] N. Martys, M. Cieplak, and M. Robbins, Phys. Rev. Lett. **66**, 1058 (1991).
[8] C. S. Nolle, B. Koiller, N. Martys, and M. O. Robbins, Phys. Rev. Lett. **71**, 2074 (1993).
[9] J. F. Gouyet, M. Rosso, and B. Sapoval, Phys. Rev. B **37**, 1832 (1988).
[10] M. Ferer, G. S. Bromhal, and D. H. Smith, Physica A **311**, 5 (2002).
[11] D. Wilkinson, Phys. Rev. A **34**, 1380 (1986).
[12] D. Stauffer and A. Aharony, *Introduction to Percolation Theory*, 2nd ed. (Taylor and Francis, Philadelphia, 1994).
[13] B. Xu, Y. C. Yortsos, and D. Salin, Phys. Rev. E **57**, 739 (1998).
[14] R. Lenormand, Proc. R. Soc. London, Ser. A **423**, 159 (1989).
[15] M. Blunt, M. J. King, and H. Scher, Phys. Rev. A **46**, 7680 (1992).
[16] A. P. Sheppard *et al.*, J. Phys. A **32**, L521 (1999).
[17] C. D. Lorenz and R. M. Ziff, Phys. Rev. E **57**, 230 (1998).
[18] M. Ferer, G. S. Bromhal, and D. H. Smith, Phys. Rev. E **71**, 026303 (2005).
[19] M. Ferer, G. S. Bromhal, and D. H. Smith, Adv. Water Resour. **30**, 284 (2006).
[20] O. I. Frette *et al.*, Phys. Rev. E **55**, 2969 (1997).
[21] C. D. Tsakiroglou, J. Non-Newtonian Fluid Mech. **117**, 1 (2004).
[22] M. Ferer, G. S. Bromhal, and D. H. Smith, Physica A **319**, 11 (2003).
[23] M. Ferer, C. Ji, G. S. Bromhal, J. Cook, G. Ahmadi, and D. H. Smith, Phys. Rev. E **70**, 016303 (2004).
[24] M. Ferer, G. S. Bromhal, and D. H. Smith, Phys. Rev. E **67**, 051601 (2003).
[25] J.-D. Chen and D. Wilkinson, Phys. Rev. Lett. **55**, 1892 (1985).
[26] R. Lenormand, E. Touboul, and C. Zarcone, J. Fluid Mech. **189**, 165 (1988).
[27] M. Sahimi and A. O. Imdakm, J. Phys. A **21**, 3833 (1988).
[28] M. Blunt and P. King, Phys. Rev. A **42**, 4780 (1990).
[29] M. Ferer, W. N. Sams, R. A. Geisbrecht, and D. H. Smith, Phys. Rev. E **47**, 2713 (1993).
[30] M. Sahimi, *Flow & Transport in Porous Media & Fractured Rock From Classical Models to Modern Approaches* (VCH Verlagsgesellschaft, Weinheim, Germany, 1994).
[31] M. Ferer *et al.*, AIChE J. **49**, 749 (1995).
[32] M. Ferer, J. C. Gump, and D. H. Smith, Phys. Rev. E **53**, 2502 (1996).
[33] E. Aker, *A Simulation for Two-Phase Flow in Porous Media* (University of Oslo, Oslo, 1996).
[34] E. Aker, K. J. Maloy, and A. Hansen, Phys. Rev. E **58**, 2217 (1998).
[35] E. Aker, K. J. Maloy, and A. Hansen, Phys. Rev. E **61**, 2936 (2000).
[36] M. Ferer and D. H. Smith, Phys. Rev. E **49**, 4114 (1994).
[37] K. Stevenson *et al.*, Physica A **367**, 7 (2006).